Direct *k*-Space Mapping of the Electronic Structure in an Oxide-Oxide Interface

G. Berner,[1] M. Sing,[1] H. Fujiwara,[2] A. Yasui,[3] Y. Saitoh,[3] A. Yamasaki,[4] Y. Nishitani,[4] A. Sekiyama,[2] N. Pavlenko,[5,6,7]
T. Kopp,[5] C. Richter,[5,7] J. Mannhart,[7] S. Suga,[8] and R. Claessen[1]

[1]*Physikalisches Institut and Röntgen Center for Complex Materials Systems (RCCM), Universität Würzburg,
Am Hubland, D-97074 Würzburg, Germany*
[2]*Division of Materials Physics, Graduate School of Engineering Science, Osaka University, Osaka 560-8531, Japan*
[3]*Condensed Matter Science Division, Japan Atomic Energy Agency, SPring-8, Hyogo 679-5148, Japan*
[4]*Faculty of Science and Engineering, Konan University, Kobe 658-8501, Japan*
[5]*Center for Electronic Correlations and Magnetism, Experimental Physics VI, Universität Augsburg, D-86135 Augsburg, Germany*
[6]*Center for Electronic Correlations and Magnetism, Theoretical Physics III, Universität Augsburg, D-86135 Augsburg, Germany*
[7]*Max Planck Institute for Solid State Research, Heisenbergstraße 1, D-70569 Stuttgart, Germany*
[8]*Institute of Scientific & Industrial Research, Osaka University, Ibaraki, Osaka 567-0047, Japan*
(Received 12 January 2013; published 12 June 2013)

The interface between $LaAlO_3$ and $SrTiO_3$ hosts a two-dimensional electron system of *itinerant* carriers, although both oxides are band insulators. Interface ferromagnetism coexisting with super-conductivity has been found and attributed to *local* moments. Experimentally, it has been established that Ti $3d$ electrons are confined to the interface. Using soft x-ray angle-resolved resonant photoelectron spectroscopy we have directly mapped the interface states in k space. Our data demonstrate a charge dichotomy. A mobile fraction contributes to Fermi surface sheets, whereas a localized portion at higher binding energies is tentatively attributed to electrons trapped by O vacancies in the $SrTiO_3$. While photovoltage effects in the polar $LaAlO_3$ layers cannot be excluded, the apparent absence of *surface-related* Fermi surface sheets could also be fully reconciled in a recently proposed electronic reconstruction picture where the built-in potential in the $LaAlO_3$ is compensated by *surface* O vacancies serving also as a charge reservoir.

Breaking the translational or inversion symmetry at surfaces and interfaces may lead to a rearrangement of charge, spin, orbital, and lattice degrees of freedom. The consequences are particularly interesting in the case of oxides, where already a slight shift in the balance of the respective interactions can stabilize one out of several competing orders or even create novel phases. The case in hand is the formation of a high-mobility two-dimensional electron system (2DES) from Ti $3d$ states at the interface of $LaAlO_3/SrTiO_3$ (LAO/STO) heterostructures [1–9] which undergoes a transition into a two-dimensional superconducting state below 0.2 K [4]. However, depending on growth conditions LAO/STO has also been found to display pronounced magnetotransport effects indicating the existence of local moments [10]. More recently, even the simultaneous presence of ferro-magnetism and superconductivity has been reported, possibly due to phase separation within the interface [11–14].

The physical origin of the 2DES formation is still debated. The observation that both interface conductivity as well as ferromagnetism only appear for a critical LAO thickness of 4 unit cells (uc) and beyond has been related to electronic reconstruction [2,13]. In this scenario electrons are transferred from the surface to the interface in order to minimize the electrostatic energy resulting from the polar discontinuity between LAO and STO [3]. Alternative explanations involve doping by oxygen vacancies [15,16]

and/or cation intermixing [17] but so far have failed to account for the critical thickness. What hampers a better understanding is the lack of microscopic information, in particular on the electronic properties of the interface and the adjacent oxide layers.

Photoelectron spectroscopy is unique in that it can directly probe the single-particle excitations of the valence electrons, which determine the low-energy properties of a solid. Regarding the Ti $3d$ interface electrons in LAO/STO, however, this is hindered for conventional photon energies in the range of 20–100 eV by the insufficient probing depth while in the hard x-ray regime the photoionization cross sections are too low. Only recently, it has been shown that the Ti $3d$ states can be detected by exploiting the resonance enhancement at the Ti L edge, i.e., by utilizing soft x rays [8,9]. Here we use soft x-ray resonant photoelectron spec-troscopy (SX-ResPES) to probe the occupied part of the electronic states and in particular its angle-resolved (AR) mode to record Fermi surface (FS) and band maps. Note that the resulting electronic structure may differ from that probed in transport measurements due to the additional presence of x-ray induced photocarriers [6,18].

The LAO/STO heterostructure with a 4 uc thick LAO overlayer was grown at the University of Augsburg by pulsed laser deposition on a TiO_2-terminated STO sub-strate. The film thickness was monitored by reflection high-energy electron diffraction (RHEED). During growth

the oxygen pressure amounted to 1×10^{-4} mbar while the substrate was held at 780 °C. Subsequently, the sample was cooled down to room temperature in 0.4 bar of oxygen. Prior to the measurements, the sample surface was cleaned by ozone and gentle *in situ* heating at 180 °C [19]. Note that for our samples it has been shown previously that the interface becomes conducting only if a critical thickness of 4 uc is reached [2] and that the highly mobile electrons [20] are confined within a few unit cells on the STO side of the interface where they occupy Ti $3d$ states [6,21,22].

The experiments were performed at the soft x-ray beam line BL23SU of SPring-8 using a photoemission spectrometer equipped with a Gammadata-Scienta SES-2002 electron analyzer [23] and the fully circularly polarized light from a helical undulator. The energy resolution was set to 110 meV for the angle-integrated and 180 meV for the angle-resolved experiments while the sample temperature was 20 K for all measurements. The angular resolution of the SX-ARPES measurements was 0.2° along and 0.5° perpendicular to the analyzer slit. The Fermi surface map was generated by integrating energy distribution curves at each k point over an interval of 0.3 eV centered around the Fermi energy. All spectra were corrected for the contribution from second order light [24]. The position of the Fermi level was determined from an *in situ* evaporated gold film [25].

The density functional calculations have been performed using the generalized gradient approximation (GGA + U) in the Perdew-Burke-Ernzerhof pseudopotential implementation [26] in the QUANTUM ESPRESSO (QE) package [27], with the local Coulomb repulsion U between Ti $3d$ electrons being 2 eV [28].

In Fig. 1(a) we show angle-integrated ResPES spectra near the chemical potential for a sample with a conducting interface (4 uc LAO) upon tuning the photon energy through the Ti L absorption edge. Exciting at a specific absorption edge makes ResPES element specific. Two processes with the same final state quantum mechanically interfere, namely, the direct photoemission and the (coherent and element-specific) Auger emission of the outer valence electrons (involving the direct recombination of a valence electron with the core hole). Thus, any enhancement of spectral weight upon tuning the energy through an absorption edge corresponds to the valence electrons of the respective atomic species, in our case Ti $3d$ states (for details on ResPES see Supplemental Material, Sec. I [25]).

The complete valence band spectrum, measured on resonance ($h\nu = 460.20$ eV), is depicted in Fig. 1(c). The off-resonance spectrum ($h\nu = 445.95$ eV) shows no spectral weight at the chemical potential. Moving through the resonance two structures appear—indicating that both are of Ti $3d$ character—a broad structure at a binding energy of ≈ 1.3 eV (A) and a structure which is cut off by the Fermi-Dirac distribution function [marked by B in Fig. 1(a)] and hence is tentatively ascribed to metallic states. Interestingly, the two features A and B resonate at
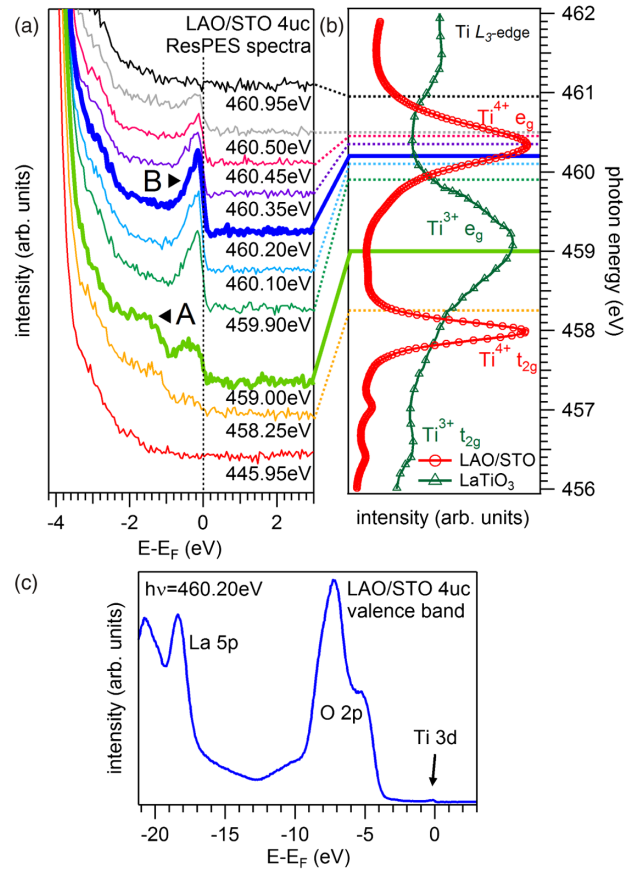

FIG. 1 (color online). (a) Angle-integrated resonant photoemission spectra upon tuning the photon energy through the Ti L absorption edge. (b) Ti L absorption spectra, recorded in total electron yield mode, of LAO/STO (red open circles) and LaTiO$_3$ (green open triangles, taken from Ref. [7]). The photon energies used in the measurements displayed in (a) are indicated by dashed and solid lines. (c) On-resonance photoemission spectrum, displaying the complete valence band.

different photon energies which already signals that they originate from different types of electronic states.

To get further insight, one has to relate the ResPES excitation energies to their positions on the resonance curve, i.e., the x-ray absorption spectrum [Fig. 1(b)]. The spectrum to compare with is that of a reference sample representative for Ti in a 3+ oxidation state, here LaTiO$_3$ (green open triangles), while for LAO/STO (red open circles) the absorption is dominated by the Ti^{4+} ions of the substrate. Peak A resonates exactly on the absorption maximum (associated with the so-called e_g levels) of LaTiO$_3$ (Ti^{3+}) whereas the maximum enhancement of B is delayed by ≈ 1 eV to almost the following absorption minimum. In addition, feature B resonates over a wider energy range than feature A. This phenomenology is known from ResPES on transition metals [29] and indicates that features A and B should originate from localized and delocalized states, respectively [25]. While the delocalized states (B) are readily identified as Ti $3d$ band states,
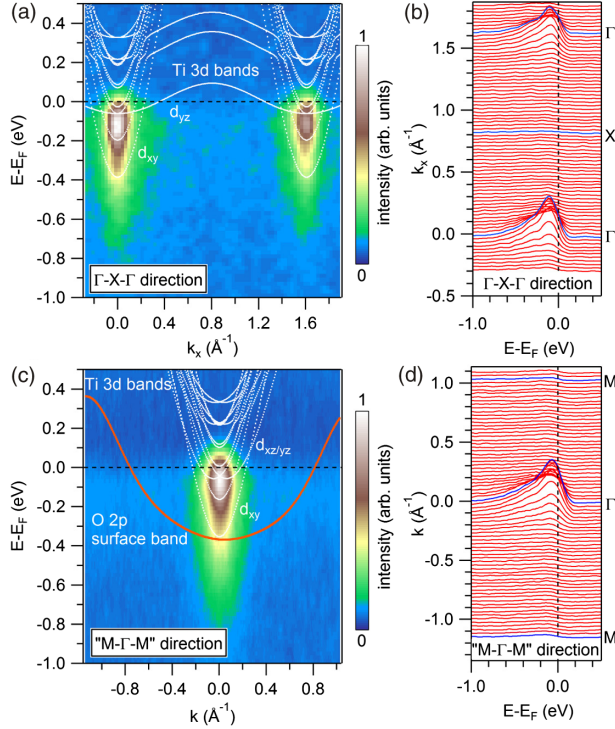
FIG. 2 (color online).   (a) Band map along the Γ-X-Γ line of the Brillouin zone (BZ). (b) Same data as in (a) depicted as energy distribution curves. (c) Band map along a cut close to the M-Γ-M line of the BZ (hence denoted by ''M-Γ-M''). (d) Same data as in (c), depicted as energy distribution curves. All data were taken at $h\nu = 460.20$ eV. White and red lines represent theoretical band dispersions (for details see text).

forming the 2DES, we assign the localized states (A) to Ti $3d$ impurity states. Such trapped states are likely to be induced by O vacancies adjacent to Ti ions. Our recent band structure calculations based on density-functional theory (DFT) reveal similar peaks in the density of states between -2 and -1 eV, depending on O vacancy configuration and concentration [14]. Similar observations have

been reported for scanning tunneling spectroscopy measurements on LAO/STO [30] and PES experiments on bare STO surfaces [31,32], where the spectral weight at the chemical potential and the in-gap states around -1.3 eV were discussed in terms of coherently screened and poorly screened excitations [32], respectively.

Since momentum information is still preserved in valence band photoemission using soft x rays and due to the resonance enhancement at the Ti L edge, we have been able to perform k-space mapping of the 2DES interface states [Figs. 2(a) and 2(c)]. In Figs. 2(b) and 2(d) we display the corresponding k-resolved energy dispersion curves along the Γ-X-Γ direction and a cut close to the M-Γ-M line [see dashed lines in Fig. 3(b)]. One clearly observes states dispersing with k around Γ and an occupied bandwidth of ≈ 0.4 eV, conclusively confirming our tentative assignment from above to the metallic interface band states of the 2DES. In Figs. 2(a) and 2(c), the electronic dispersions of DFT calculations are overlaid. The calculations fairly reproduce the experimental bandwidth, while the experimental broadening does not allow us to resolve all the individual quantum well states owing to the confinement of the 2DES [33], although the energy distribution curves in Figs. 2(b) and 2(d) indicate the existence of at least two bands.

Additional information can be extracted from the FS map in Fig. 3. An essentially isotropic distribution of high intensity centered at the Γ points of the Brillouin zone (BZ) of STO is observed. Superimposed one finds, with much lower intensity, flower-shaped spectral weight with the lobes directed towards the X points of the BZ and stretching further out than the isotropic intensity distribution as is most clearly seen around the lower left Γ point in Fig. 3(a). These observations are in line with the FS sheets from the DFT calculations which are overlaid on top of the PES data in Fig. 3(b). Note, however, that the experimental Fermi surface volume might be slightly enhanced due to photogenerated charge carriers [6]. The calculations
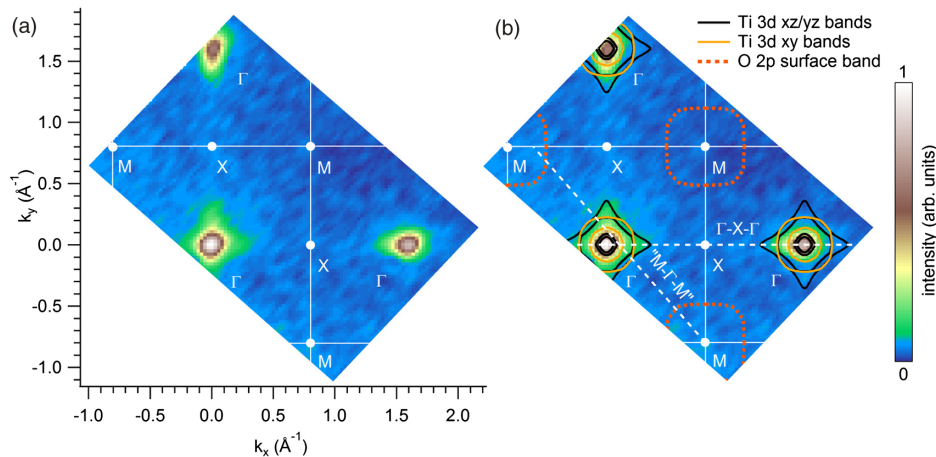

FIG. 3 (color online).   (a) FS map recorded at $h\nu = 460.20$ eV. (b) Same map as (b) but with the cuts in the BZ corresponding to the data in Figs. 2(a)–2(d) indicated and the FS sheets from DFT calculations overlaid.

further reveal that the isotropic intensity distribution originates mainly from light Ti $3d_{xy}$ bands while the flower-shaped intensity distribution is due to heavy d_{xz}/d_{yz} [Fig. 2] bands, similar to what has recently been reported for a 2DES at the surface of bare STO [33].

However, there is also a striking discrepancy between experiment and theory. In the calculations, which are performed for stoichiometric samples, i.e., in the absence of oxygen vacancies in the LAO, a holelike FS is predicted around the M points as indicated by the orange dashed lines in Fig. 3(b). It is due to the Fermi level crossing of O $2p$ derived states from the valence band maximum of the topmost monolayer of the LAO film. Since the photoelectron current emitted from the surface is hardly damped by scattering events and since the band is almost completely filled, these hole pockets, if existing, should be observable even without resonance enhancement. In the standard electronic reconstruction scenario [Fig. 4(a)] the polarity-induced potential buildup across the overlayer gradually shifts the valence band of LAO towards the Fermi level. At the critical thickness, the valence band maximum crosses the Fermi level which gives rise to the hole pockets predicted by the DFT calculations, while the released electrons populate the lowest lying Ti $3d$ states at the STO side of the interface [34].

From the obvious absence of metallic surface bands we conclude that the potential difference is (almost completely) screened out in the LAO film [35]. A possible explanation could be that under illumination electron-hole pairs are created which get separated by the initial polarization field in the LAO [Fig. 4(b)]. Eventually, depending on the rates for electron-hole pair creation and recombination, a dynamic equilibrium will be established where the opposing electric field due to the separated electron-hole pairs just cancels the initial field, thus prohibiting the observation of the surface related hole pocket. On the other hand, in another heterostructure with an interface between a polar and a nonpolar material ($LaCrO_3/SrTiO_3$) a built-in potential has readily been identified by x-ray photoelectron

spectroscopy (XPS) with a similar potential drop per unit cells as predicted for LAO/STO in the standard electronic reconstruction scenario [36].

Looking for alternative explanations, our SX-ARPES results could also be fully reconciled within recent proposals, also based on DFT calculations, that oxygen vacancies at the LAO surface can serve as a charge reservoir for the electronic reconstruction [37–40]. In such a scenario the O vacancies induce unoccupied in-gap states, which due to possible disorder of the vacancies in the real system might easily become localized. The released two electrons per O vacancy are transferred to the interface by the LAO polar field. This field is thereby efficiently reduced [see Fig. 4(c)], in line with XPS measurements which show no core-level broadening or shift with film thickness [41].

Viewing the LAO film as a parallel plate capacitor the energy gain per charge transferred from the surface to the interface increases linearly with film thickness. While the energy costs for the creation of oxygen vacancies can depend also on thickness (and in addition on vertical position), the calculations show that at a certain thickness it becomes on balance favorable to create an oxygen vacancy at the surface and transfer the released electrons to the interface [37–40]. Note that O vacancies in the STO can be excluded with fair certainty as a source of electrons for the 2DES. First, their density essentially does not depend on film thickness but on the growth conditions and so the critical thickness behavior as observed in our samples could hardly be explained [2]. Second, in our data the electrons associated with O vacancies in the STO (feature A) are well separated and far below the 2DES related states at the chemical potential (feature B) and thus cannot populate the 2DES related states.

Summarizing our results we arrive at the picture that at the conducting interface besides heavy Ti $3d_{xz/yz}$ and light Ti $3d_{xy}$ bands there also exist *localized* charge carriers of Ti $3d$ character. These are probably trapped by adjacent O vacancies, i.e., O vacancies in the STO at the interface. It is hence tempting to associate the trapped and mobile interface charge with ferromagnetism and superconductivity, respectively [14], which both have recently been reported to coexist at the interface. As a matter of fact, the hallmarks of the microscopic view of the standard electronic reconstruction scenario—a metallic surface and a potential drop across the LAO overlayer of the order of the STO band gap—have experimentally remained elusive so far. Our data clearly indicate that they are absent in our spectroscopic experiments. Modified electronic reconstruction scenarios involving surface O vacancies as a charge reservoir could explain these findings. Since we cannot rule out the possibility that the LAO polar field is screened out by a photo-induced reverse voltage our results call for both a systematic investigation of scenarios taking O vacancies into account and combined *in situ* transport and spectroscopy experiments. In any case, these results demonstrate for the first
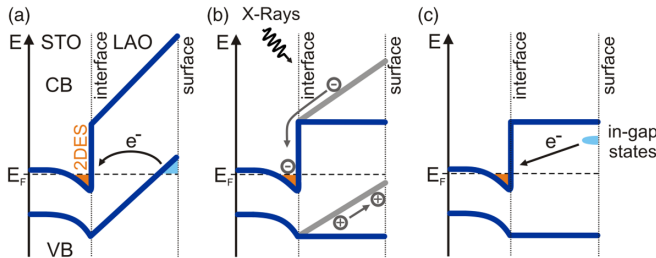

FIG. 4 (color online). (a) Schematic band diagram for the standard electronic reconstruction scenario in LAO/STO. (b) Possible situation where the polarization field in the LAO is screened by the separation of electron-hole pairs created upon illumination with x rays. (c) Tentative band situation with the inclusion of O vacancies at the LAO surface as a charge reservoir for electronic reconstruction.

---

[1] A. Ohtomo and H. Y. Hwang, Nature (London) **427**, 423 (2004).

[2] S. Thiel, G. Hammerl, A. Schmehl, C. W. Schneider, and J. Mannhart, Science **313**, 1942 (2006).

[3] N. Nakagawa, H. Y. Hwang, and D. A. Muller, Nat. Mater. **5**, 204 (2006).

[4] N. Reyren et al., Science **317**, 1196 (2007).

[5] M. Basletic, J.-L. Maurice, C. Carrétéro, G. Herranz, O. Copie, M. Bibes, É. Jacquet, K. Bouzehouane, S. Fusil, and A. Barthélémy, Nat. Mater. **7**, 621 (2008).

[6] M. Sing et al., Phys. Rev. Lett. **102**, 176805 (2009).

[7] M. Salluzzo et al., Phys. Rev. Lett. **102**, 166804 (2009).

[8] G. Drera et al., Appl. Phys. Lett. **98**, 052907 (2011).

[9] A. Koitzsch, J. Ocker, M. Knupfer, M. C. Dekker, K. Dörr, B. Büchner, and P. Hoffmann, Phys. Rev. B **84**, 245121 (2011).

[10] A. Brinkman, M. Huijben, M. van Zalk, J. Huijben, U. Zeitler, J. C. Maan, W. G. van der Wiel, G. Rijnders, D. H. A. Blank, and H. Hilgenkamp, Nat. Mater. **6**, 493 (2007).

[11] L. Li, C. Richter, J. Mannhart, and R. C. Ashoori, Nat. Phys. **7**, 762 (2011).

[12] J. A. Bert, B. Kalisky, C. Bell, M. Kim, Y. Hikita, H. Y. Hwang, and K. A. Moler, Nat. Phys. **7**, 767 (2011).

[13] B. Kalisky, J. A. Bert, B. B. Klopfer, C. Bell, H. K. Sato, M. Hosoda, Y. Hikita, H. Y. Hwang, and K. A. Moler, Nat. Commun. **3**, 922 (2012).

[14] N. Pavlenko, T. Kopp, E. Y. Tsymbal, G. A. Sawatzky, and J. Mannhart, Phys. Rev. B **85**, 020407 (2012).

[15] A. Kalabukhov, R. Gunnarsson, J. Börjesson, E. Olsson, T. Claeson, and D. Winkler, Phys. Rev. B **75**, 121404 (2007).

[16] W. Siemons, G. Koster, H. Yamamoto, W. A. Harrison, G. Lucovsky, T. H. Geballe, D. H. A. Blank, and M. R. Beasley, Phys. Rev. Lett. **98**, 196802 (2007).

[17] P. R. Willmott et al., Phys. Rev. Lett. **99**, 155502 (2007).

[18] It is known that ultraviolet light illumination with energies exceeding the STO band gap causes photoconductivity in LAO/STO samples [M. Huijben, G. Rijnders, D. H. A.

Blank, S. Bals, S. Van Aert, J. Verbeeck, G. Van Tendeloo, A. Brinkman, and H. Hilgenkamp, Nat. Mater. **5**, 556 (2006)]. Using even higher photon energies in SX-PES obviates the need for keeping the samples in the dark prior to the experiments as is done, e.g., in transport measurements to avoid photocarrier contributions.

[19] See Supplemental Material at http://link.aps.org/supplemental/10.1103/PhysRevLett.110.247601 for Sec. III.

[20] C. W. Schneider, S. Thiel, G. Hammerl, C. Richter, and J. Mannhart, Appl. Phys. Lett. **89**, 122101 (2006).

[21] G. Berner et al., Phys. Rev. B **82**, 241405 (2010).

[22] K.-J. Zhou, M. Radovic, J. Schlappa, V. Strocov, R. Frison, J. Mesot, L. Patthey, and T. Schmitt, Phys. Rev. B **83**, 201402 (2011).

[23] Y. Saitoh et al., J. Synchrotron Radiat. **19**, 388 (2012).

[24] See Supplemental Material at http://link.aps.org/supplemental/10.1103/PhysRevLett.110.247601 for Sec. II.

[25] See Supplemental Material at http://link.aps.org/supplemental/10.1103/PhysRevLett.110.247601 for Sec. I.

[26] J. P. Perdew, K. Burke, and M. Ernzerhof, Phys. Rev. Lett. **77**, 3865 (1996).

[27] P. Giannozzi et al., J. Phys. Condens. Matter **21**, 395502 (2009).

[28] See Supplemental Material at http://link.aps.org/supplemental/10.1103/PhysRevLett.110.247601 for Sec. IV.

[29] T. Kaurila, J. Väyrynen, and M. Isokallio, J. Phys. Condens. Matter **9**, 6533 (1997).

[30] Z. Ristic, R. Di Capua, F. Chiarella, G. M. De Luca, I. Maggio-Aprile, M. Radovic, and M. Salluzzo, Phys. Rev. B **86**, 045127 (2012).

[31] Y. Aiura, I. Hase, H. Bando, T. Yasue, T. Saitoh, and D. S. Dessau, Surf. Sci. **515**, 61 (2002).

[32] Y. Ishida, R. Eguchi, M. Matsunami, K. Horiba, M. Taguchi, A. Chainani, Y. Senba, H. Ohashi, H. Ohta, and S. Shin, Phys. Rev. Lett. **100**, 056401 (2008).

[33] A. F. Santander-Syro et al., Nature (London) **469**, 189 (2011).

[34] R. Pentcheva, and W. E. Pickett, Phys. Rev. Lett. **102**, 107602 (2009).

[35] The leading edge of the O 2*p*-derived states (originating from both LAO and STO) in Fig. 1(b) indicates an energy gap of about 3.2 eV, corresponding within experimental accuracy to the STO band gap. If there was a sizable potential difference across the LAO left, the gap of the leading edge (then originating solely from LAO) would have to be significantly reduced.

[36] S. A. Chambers, L. Qiao, T. C. Droubay, T. C. Kaspar, B. W. Arey, and P. V. Sushko, Phys. Rev. Lett. **107**, 206802 (2011).

[37] Z. Zhong, P. X. Xu, and P. J. Kelly, Phys. Rev. B **82**, 165127 (2010).

[38] N. C. Bristowe, P. B. Littlewood, and E. Artacho, Phys. Rev. B **83**, 205405 (2011).

[39] Y. Li, S. N. Phattalung, S. Limpijumnong, J. Kim, and J. Yu, Phys. Rev. B **84**, 245307 (2011).

[40] N. Pavlenko, T. Kopp, E. Y. Tsymbal, J. Mannhart, and G. A. Sawatzky, Phys. Rev. B **86**, 064431 (2012).

[41] Y. Segal, J. H. Ngai, J. W. Reiner, F. J. Walker, and C. H. Ahn, Phys. Rev. B **80**, 241107 (2009).